# Mineral Mapping of the Lunar Surface Using Chandrayaan-1 Hyperspectral Imager (HySi) and Moon Mineralogy Mapper (M³) Hyperspectral Data

Mohammed Zeeshan R.[1], Ajit Kumar[1], Sayyad S. B.[1], Deshmukh R. R.[2]

[1]Milliya Arts, Science & management Science College, Beed (MS) India -431122

[2]Department of Computer Science & IT, Dr. Babasaheb Ambedkar Marathwada University, Aurangabad (MS) India -431001

**Abstract:**

**The Hyperspectral data provides a platform to discriminate different minerals on the lunar surface which leads to better understand the origin, evolution, and composition on the surface of the moon. Compositional mapping of the lunar surface is considered as a standard approach for mineral mapping. This paper reports surface mineralogy of the lunar surface from Mare Crisium using Chandrayaan-1 Hyperspectral remotely sensed data from HySi sensor. Because of the limited coverage of HySi, a comparative study of the same area is carried out using data from on board Chandrayaan-1 Moon Mineralogy Mapper (M³) which provides VIS-NIR spectral data of the lunar surface. False color composites is created using different band shaping algorithms like band strength, band curve and band tilt parameters at crucial wavelength for spatial analysis. Spectral analysis has been done from derived reflectance spectra from both data sets. Spectral reflectance obtained from M³ sensor helps to confirm the mineralogy on the area under study. The result reveals different categories of minerals which are high-Ca pyroxene (Clinopyroxene), olivine and low Ca-pyroxene (Orthopyroxene).**

**KEY WORDS:** Hyperspectral Imager (HySi), Band Strength, Band Curve, Band Tilt

## 1. Introduction

Imaging spectroscopy considered to be a useful approach for understanding the composition of the earth and planetary bodies. It provides data in narrow continuous bands with fine spectral and spatial resolutions. An approach based on color differences has been used as a primary technique to study the composition of the earth and planetary surfaces. Compositional mapping of the lunar surface can be done by examining the reflectance spectra derived from the hyperspectral data. The moon mineral can be well distinguished in visible to near infrared region of the spectrum by characteristic absorption bands [1].the diagnostic absorption features for specific minerals are generally prominent in the near infrared region of the spectrum [2]. The particular diagnostic Features at different wavelengths across the electromagnetic spectrum is mainly because of electronic transitions and vibrational processes [3]. The shape and strength of the absorption and the wavelength position across the spectrum is depends on compositional structure of the mineral [4-6]. Mineral mapping of the lunar surface provides an opportunity to better understand the origin, evolution and geological history of the moon [7]. The iron bearing silicate minerals like olivine and pyroxene which are the most abundant mafic minerals have electronic transition absorption band due to ferrous ion at near infrared wavelengths [8]. The Fig. 1 shows the reflectance spectra of common mafic minerals. The most common mafic minerals are pyroxene [9] and olivine has characteristic absorption in the near infrared region which varies with the composition of the mineral [10]. The mineralogy of the lunar surface from different lithological areas helps to predict the material composition.

Many satellite missions has flown to moon for different objectives and applications. The Moon Mineralogy Mapper (M³) [8] and Hyperspectral Imager (HySi) [11] onboard Chandrayaan-1, The India's first mission to moon [12] provides hyperspectral data of the lunar surface. This paper demonstrates the compositional mapping of lunar surface to identify lunar surface minerology using Hysi and M³ hyperspectral data which helps to understand the crustal composition of the lunar surface. A comparative study of the selcted area is carried out using data from the mentioned hyperspectral sensors out of which the M³ sensor provides contineous data with better spectral coverage that helps to discriminate among different minerals such as High-Ca pyroxene and olivine both have strong absorption near 1000 nm, plagioclase has absorption at 1250 nm which is quite ambigous in case of HySi data due to its limited spectral coverage.
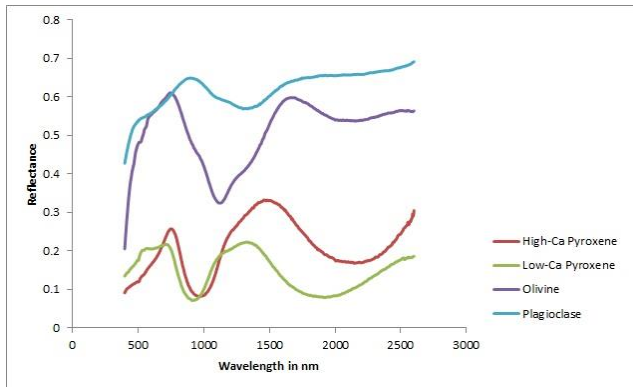
**Figure 1.** Reflectance Spectra of Typical Lunar Minerals (Adams,1974).

## 2.The Study Area

The mare Crisium is located at the near side of the moon and centered at 17° N and 60° E. The Main ring diameter is 740 km and the basin depth is 4.57 km the Mare Crisium is a multi-ring basin has 555 km in diameter. It is having flat floor and ring of wrinkle ridges at its outer boundaries.
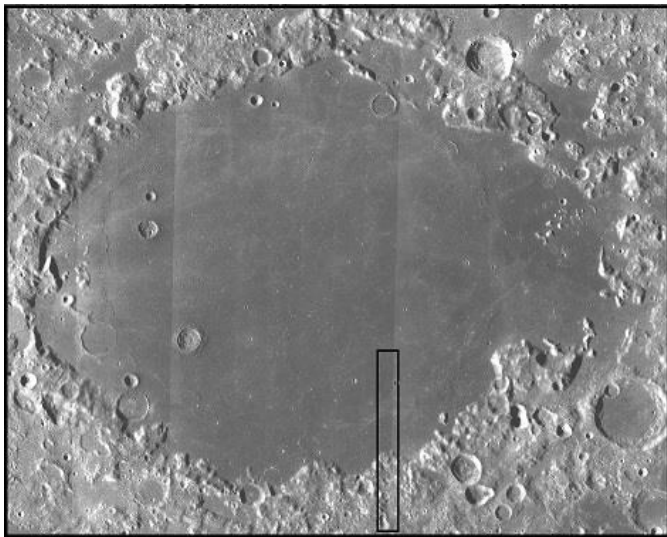


**Figure 2.** Hysi and M$^3$ Coverage Shown on LRO LROC WAC Image.

## 3. Materials and Method

Hyperspectral Data from Hyperspectral Imager (Hysi) Sensor and Moon Mineralogy Mapper (M$^3$) Onboard Chandrayaan-1 for mineral mapping in the southern part of mare Crisium was used in this study. The Hysi sensor records the data in pushbroom mode covering 430-964 nm having 64 contineous bands with the spectral resolution of 15 nm and spatial resolution of 80 m with 20 km swath[11]. Band to band registered level-4 Hysi image was downloaded from issdc.gov.in. The image subset covering the study area from orbit number 684 with product Id HYS_NREF_20090104T161501992 and data set from M$^3$ was a guest instrument of NASA onboard Chandrayaan-1 [10].the sensor records the data in push broom mode and the spectral

coverage is 400 nm to 2900 nm with 84 spectral bands with 20-40 nm bandwidth and the spatial resolution is 140-280 meters [8]. The data set was downloaded from PDS geosciences node lunar orbital data explorer (www.ode.rel.wustl.edu/moon) with product id m3g20090104t161446_v01_rfl.shown in Fig (3). Environment for visualizing images (ENVI) software was used for processing, analyzing and deriving spectra from varying locations for both data sets. The Band to band registered level-4 HySi data has been used for the study. The data product was opened in Envi software by defining new header and The BBR-4 level hysi data then converted to apparent reflectance using spectral math tool. The data set was geometrically corrected using geometry information provided with the data set. The spatial subset of the Hysi image is considered covering the southern part of the area under study shown in fig 3(a). photometrically calibrated reflectance data (REFIMG)  from Moon Mineralogy Mapper (M3) was downloaded and spatial  subset pertaining to study area was obtained as shown in fig 3(b).
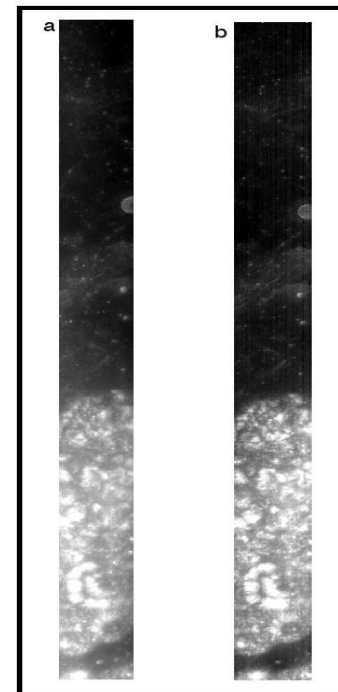


**Figure 3.** (a) HySi reflectance image band 15, (b) M$^3$ reflectance image band 15.
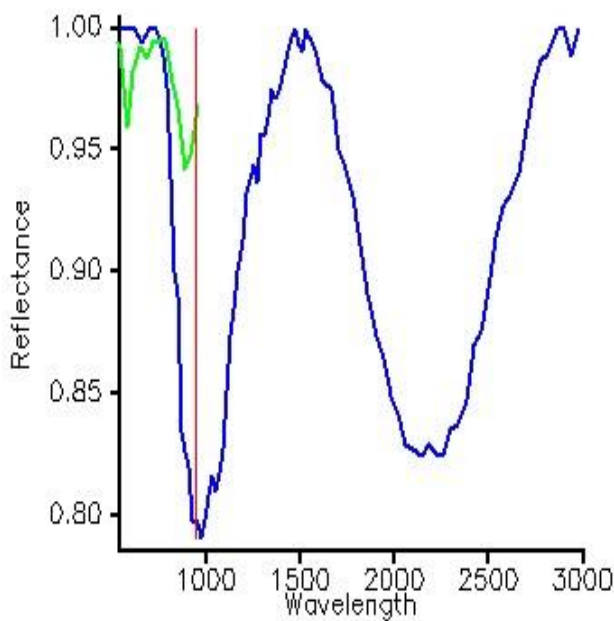
**Figure 3.** (c) Spectral profile derived from HySi in green superimposed on M3 spectra in blue showing the spectral coverage of both sensors.

### 3.1 Mineral mapping using Band shaping algorithm

The band parameter mapped spectral and spatial variation more easily then the qualitative assessment .The use of different Spectral band parameters for Compositional mapping of lunar surface is a standard technique [13-19]. there are three band parameters which was originally derived for UV-VIS data later extended and applied on the Hysi data by [20] using HySi data for lithological mapping of the lunar surface for mare Mascovience and identified different lithological units based on different mafic minerals. The approach has also been employed on the M3 data to discriminate the specific minerals and it also provides a mechanism for clustering similar pixels together and helps to derive the spectral reflectance effectively across the study area [21] The band parameters are band strength; band curve and band tilt which is used primarily for mapping the mafic minerals on the lunar surface. The following section gives the detail about the band parameters.

### 3.1.1 Band Strength

The band strength parameter helps to estimate the abundance of the mafic minerals by the analyzing the strength of the 1000 nm absorption band. the band strength parameter for clementine data by [8] which was originally derived for clementine data is given by the following equation and later due to the band limitation of hyperspectral imager sensor it was modified by [19] and for M3 data the curvature is derived by [21] The band strength is directly related to the depth of the absorption band and it is indicative of

the relative presence of the mafic minerals and insensitive to the type of minerals. Areas with high values of BS parameter showing anorthosite and mature soil with a weak ferrous band where as strong ferrous band for unweathered areas have low bs values. In the color composite the BS parameter is assigned to blue channel. Thus the weathered and well developed soil appears in dark shades of blue and the fresh area with mafic mineral will not appear in significant blue shades. The band strength parameter can be derived for HySi and $M^3$ data set using equation (1) and (2) respectively.

$$BS = R_{947.7}/R_{748.3} \quad ----(1)$$

$$BS = R_{1008}/R_{750} \quad ----(2)$$

### 3.1.2 Band Curve

The band curvature is indicative of the type of the mafic mineral present and it is specifically sensitive to pyroxene composition. This parameter can be derived using hysi bands by the following equations suggested by [22] with minor modification according to HySi and $M^3$ bands. the curve decreases from low Ca pyroxene LCP bearing noritc rock to high Ca pyroxene HCP bearing gabbroic rock and it is further decreases for the olivine dominant rocks. The spectral Curve increases towards the longer wavelength as the wavelength of the absorption band moves towards the longer wavelengths. thus areas with LCP have high values in BC and areas with HCP having low curvature values and areas rich in olivine has very low curvature values[15]. Thus in the false color composite this parameter is assigned to red channel, the areas rich in LCP appears red to pink. The equation (3) and (4) gives formulation for band curvature using Hysi and $M^3$ respectively.

$$BC = (R_{748.3}/R_{906.3}) + (R_{947.7}/R_{906.3}) \quad ---(3)$$

$$BC = (R_{748.3}/R_{906.3}) + (R_{947.7}/R_{906.3}) \quad ---(4)$$

### 3.1.3 Band Tilt

The band tilt parameter is the intensity ratio and it is complementary to the band curvature as shown in the expression. The high values of band tilt show the area which is abundance of Clinopyroxene and olivine. The parameter defined by [15] as difference in reflectance at crucial wavelengths and later modified by [23] as the ratio of 900 nm and 1000 nm. The formulation was implemented on the Hysi data by [20] and due to the band limitations of Hysi it is further modified as in given in the

equation (5). For M3 bands the band tilt parameter was derived by [24] and it is given in equation (6).

$$BS = R_{898.0}/R_{947.7} \quad --- (5)$$

$$BS = R_{910}/R_{1008} \quad --- (6)$$

*3.1.4 Spectral reflectance analysis*

The spatial subset of the Hysi and $M^3$ image was obtained covering the southern part of the area under study. Fig. 4 shows the subset of the Hysi and $M^3$ image where the mare and highland boundary have been marked.the ENVI image processing application software was used for calculating band parameters creating false color composite. The areas in different colors are the reflectance spectra sampling locations. Around 50 reflectance spectra of 3x3 pixel averages were derived from spatially varying locations and only 16 representative spectra were selected for further analysis. For reflectance spectra derived from $M^3$ data set the Automatic straight-line approximation continuum removal Method was used for removing the continuum [25, 26] for better representation and analysis and to filter the residual absorption band shapes. The average reflectance spectra from the spatially and spectrally varying areas are shown in different color boxes has been derived from the HySi and $M^3$ data. Fig. (4) Shows the reflectance spectra from the highlighted areas.
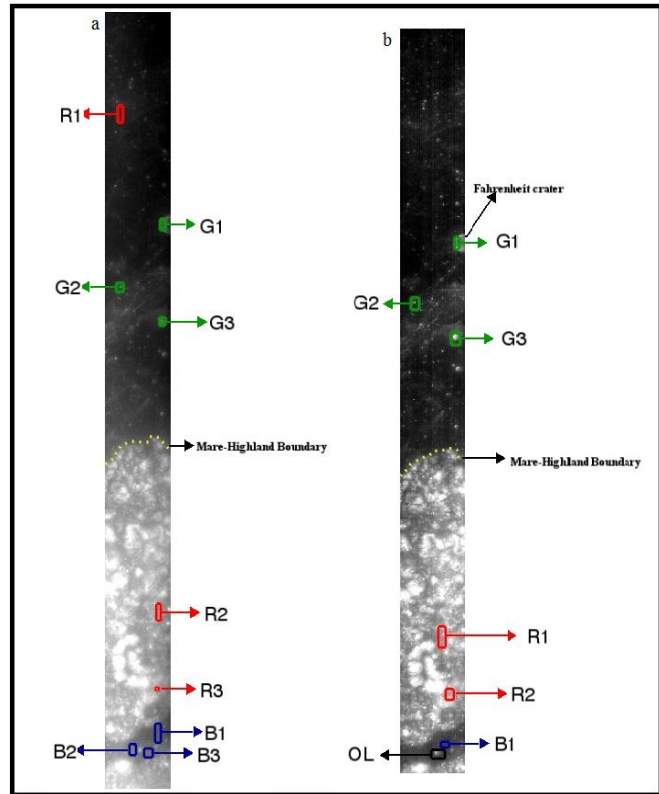


**Figure 4.** (a)Hysi Image and (b) $M^3$ image Covering study area and the Representative locations from where the reflectance spectra has been derived.

## 6. Results and Discussion

Fig (5) shows the reflectance spectra scaled at 748.3 nm derived from HySi and fig (6) and (7) shows the continuum- removed reflectance spectra obtained from $M^3$ data set from the marked areas as discussed in previous section. fig (8) shows the resultant image from the ratio of 2018 nm and 1008 nm, the area appearing bright in the grayscale image indicating the probable assemblages of olivine rich minerals as suggested by [21 and 22] and can be observed at the highland area in the lower part of the image. Fig. 9 shows the color composite images derived from HySi and $M^3$ data sets using different band shaping algorithms    and. high band strength values are appearing in shades of blue color  indicating weathered rich rocks/Anorthositic where blue color from highland (lower part of the image) showing lack of 1000 nm absorption represented by R2 and R3 areas and the spectra for the same areas can be seen in Fig (5)  where steep slope can be observed probably because of the effect of space weathering which leads to reddened slope. Similar steep slope can also be seen from mare area R1 as similar to the highland spectra R2 and R3.  Space weathered area shows high band strength values [24]. The spectra derived from $M^3$ image represented by R1 and R2 areas from fig 4(b) and the continuums-removed reflectance spectra for the areas shown in fig (7) indicating weak or no absorption near 1000 nm and the strong absorption near 2000 nm probably due to the presence of Fe-Mg-spinel [27, 28 and 29].
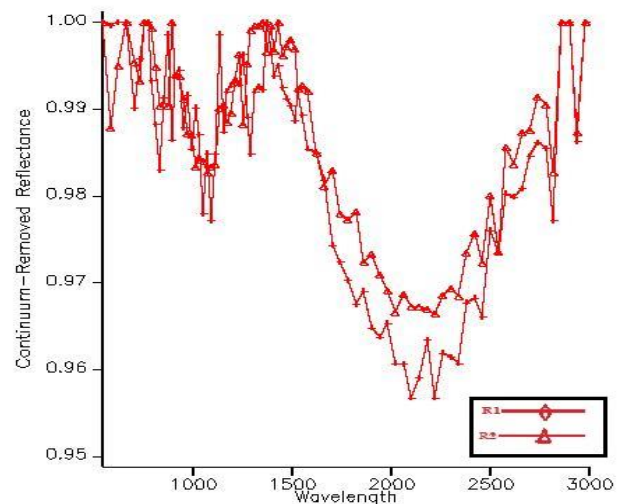
The High values of band curvature indicate the presence of LCP rich areas which appears in the shades of red to pink. The areas B1, B2 and B3 at the lower part of the composite and the spectra derived from the area can be seen in Fig. (5). shows strong absorption feature near 900 nm indicative of (orthopyroxene) LCP rich noritic rocks at the lower part of the color composite image. Whereas the same area in M$^3$ scene represented by B1 and the reflectance spectra showing strong absorption near 1000 nm and 2000 nm in fig (7) is also indicating the presence of LCP rich area however the color composite of the M$^3$ does not shows the significant red to pink component as in it appears in case of HySi color composite indicated in fig (9).



**Figure 7.** Reflectance spectra derived from R1 and R2 areas from M$^3$ image
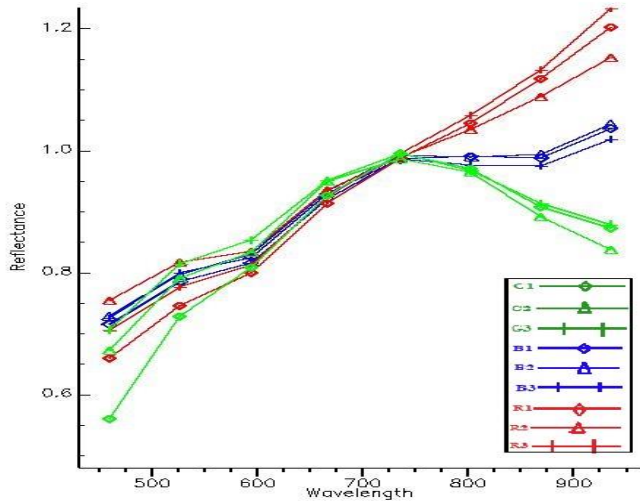


**Figure 5.** Reflectance spectra derived from different areas scaled at 748.3 nm from HySi image.
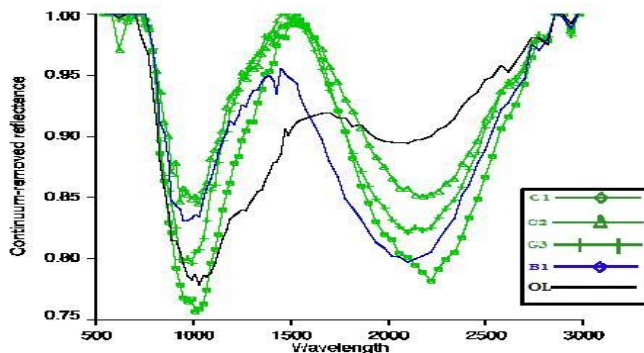


**Figure 6.** Reflectance spectra derived from different areas from M$^3$ image.

The Higher band tilt values appearing in the shades of green to yellow from the area G1,G2 and G3 from Fig 9(a) there are many small craters appearing in green to yellow. Spectral reflectance from these areas shows strong absorption going towards the longer wavelengths indicating the probable presence of high-Ca pyroxene (clinopyroxene) or olivine or plagioclase represented by spectra G1,G2 and G3 in fig (5). However data at longer wavelength is required to confirm the characteristic absorption but here on the basis of the color composite and the reflectance spectra shows the mafic rich areas. On the other hand the areas G1,G2 and G3 from M$^3$ image as shown in fig 4(b) and the spectral profile from these areas can be seen in fig (6) by G1,G2 and G3 areas respectively. The high-Ca pyroxene (HCP) mineral is identified with the absorption around 1000 nm and 2300 nm. The unweathered areas and the freshly exposed small young craters have large values of band tilt parameter. Thus the area appears green to yellow in the false color composite represents area rich in HCP (Clinopyroxene).

the spectra G1,G2 and G3 in fig(5) as already discussed shows str ong absorption towards 1000 nm however to confirm this the spectra from M$^3$ in fig (6) shows the high-ca pyroxene rich areas. thes pectra OL from fig (6) shows strong absorption near 1000 nm and no significant absorption near 2000 nm showing the presence of Olivine.[30].the lower part of the color composite in fig 9(a) appears in deep pink color indicating noritic composition and the spectra B1,B2 and B3 also shows an absorptions near 900 nm confirming the LCP rich areas however in the color composite in fig 9(b) the pink component is not significant however the spectra derived from B1 region shows the absorption at 1000 nm and 2000 nm wavelength regions by spectra B1 in fig (6).
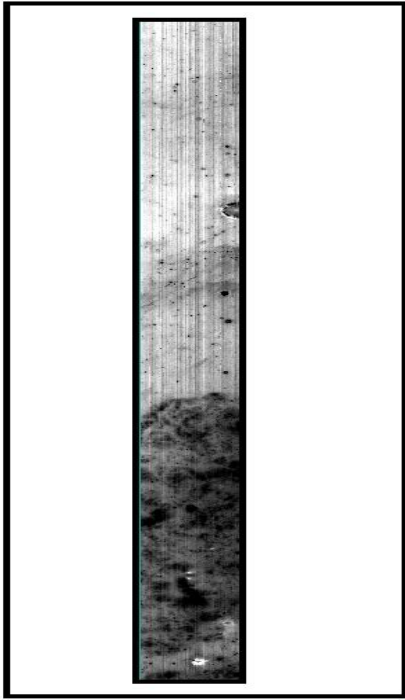
**Figure 8.** The gray scale image of ratio 2018 nm /1008 nm.
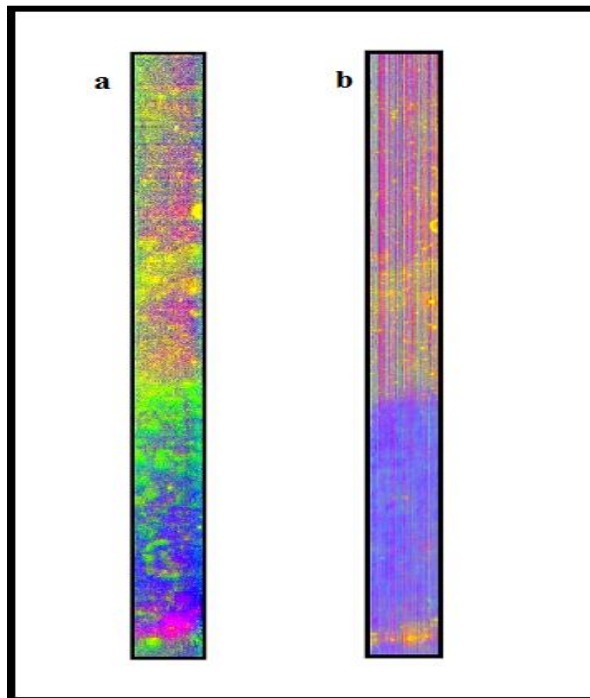


**Figure 9.** False Color Composite of HySi and M³ images using BC, BT and BS assigned to RGB respectively.

## Conclusion

A comparative analysis of the lunar surface mineralogy using HySi and M³ data was carried out in southern part of mare Crisium. Band shape parameters and their composite is an efficient approach towards mineral mapping and employed on both data sets. The spectral profile analysis for particular mineral is useful in mineral identification. The hySi data reveals the Areas rich in low-Ca pyroxene mineral have been identified. Small fresh high-Ca pyroxene craters are distinct in the mare region of the false color composite image is prominent in color composite of data sets. In case of HySi Spectra having no absorption around 900 nm with steep slopes could be because of high space weathered soil. Spectra with strong absorption around 900 nm indicating olivine and/or high Ca-pyroxne and/or plagioclase, due to limited spectral coverage of HySi, data from M3 sensor was used and the spectral reflectance derived from M³ data and color composite is created to discriminate different minerals and the spectral profile analysis gives the clear picture with characteristic diagnostic absorptions at crucial wavelength which confirms the mineralogy in the area under study and it is found that the results from both data sets are in accordance.

## References:

1.  Burns, R. G., (1970) Mineralogical Applications of Crystal Field Theory, Cambridge University Press, New York,
2.  Pieters, C. M. (1986), Composition of the lunar highland crust from near infrared spectroscopy, Rev. Geophys., 24(3), 557 – 578, doi:10.1029/RG024i003p00557.
3.  Burns, R. G. (1993). Mineralogical applications of crystal field theory (Vol. 5). Cambridge University Press
4.  Kramer, G.Y. (2010). Characterizing bedrock lithologies using small crater rim and ejecta probing (SCREP). Advances in Space Research. 45 (10), 1257–1267.
5.  Anbazhagan, S. and Arivazhagan, S. (2009) Reflectance spectra of analog basalts; implications for remote sensing of lunar geology. Planet. Space Sci., v.57, no.12, pp.1346-1358.
6.  Anbazhagan, S. and Arivazhagan, S. (2010) Reflectance spectra of analog anorthosites: Implications for lunar highland mapping. Planet. Space Sci., v.58, no.5, pp.752-760.
7.  Jin, S., Arivazhagan, S. and Araki, H. (2013) New results and questions of lunar exploration from SELENE, Chang'E-1, Chandrayaan-1 and LRO/LCROSS. Adv. Space Res., v.52,no.2, pp.285-305.

8. Tompkins, S., Pieters, C.M., (1999). Mineralogy of the lunar crust: Results from Clementine. Meteor. Planet. Sci. 34, 25–41.

9. Adams J B (1974) visible and near infrared diffuse reflectance spectra of pyroxene as applied to remote sensing of solid objects in the solar system. j geophys. res 79,4829-4836

10. Green, R. O. et al., (2011).The Moon Mineralogy Mapper (M3) imaging spectrometer for lunar science: instrumentation, calibration, and on-orbit measurement performance. J. Geophys. Res., 116, E00G19

11. Kiran Kumar, A.S., Roy Chowdhury, A., Banerjee, A., Dave, A.B., Sharma, B.N., Shah, K.J., Murali, K.R., Mehta, S., Joshi, S.R., Sarkar, S.S., (2009). Hyper Spectral Imager for lunar mineral mapping in visible and near infrared band. Curr. Sci. 96 (4),496–499.

12. Goswami, J.N., Annadurai, M., (2009). Chandrayaan-1: India's first planetary science mission to the Moon. Lunar Planetary Science (CDROM) 40, 2571

13. Sunshine, J.M., Pieters, C.M., (1993). Estimating modal abundances from the spectra of natural and laboratory pyroxene mixtures using the modified Gaussian model. J. Geophys. Res. 98, 9075–9087. doi:10.1029/93JE00677.

14. Isaacson, P.J., Pieters, C.M., (2009). Northern Imbrium Noritic Anomaly. J. Geophys. Res. 114, E09007. doi:10.1029/2008JE003293

15. Pieters, C.M., Gaddis, L., Jolliff, B., Duke, M., (2001). Rock types of South Pole-Aitken basin and extent of basaltic volcanism .J. Geophys. Res. 106,28001-28022.doi:10.1029/2000JE001414.

16. Mccord T.B and Adams J. B(1973) progress in remote optical analysis of lunar surface composition The Moon 7,453-474

17. Tompkins, S., Pieters, C.M., Mustard, J.F., Pinet, P.C., Chevrel, S.D., (1994). Distribution of materials excavated by the lunar crater Bullialdus and implications for the geologic history of the Nubium Region. Icarus 110, 261–274.

18. Lucey, P.G., Hawke, B.R., Pieters, C.M., McCord, T.B., (1981). Multispectral unit mapping of the Aristarchus region of the Moon. Bull. Am. Astron. Soc. 13, 711.

19. Pieters, C.M., Ham, S., McCord, T.B., (1980). Near-infrared lunar spectra: Patterns in the increasing data set. Lunar Planet. Sci. XI, 879–881.

20. Bhattacharya, S., Chauhan, P., Rajawat, A. S., Ajai and Kiran Kumar, A. S.,(2011). Lithological mapping of central part of Mare Moscoviense using Chandrayaan-1 Hyperspectral Imager (HySI) data.

21. Sivakumar, V., Neelakantan, R., (2015). Mineral mapping of lunar highland region using Moon Mineralogy Mapper (M3) hyperspectral data. Journal of the Geological Society of India 86 (5), 513e518

22. Borst, A.M., Foing, B.H., Davies, G.R., Van Western, W., (2012).Surface mineralogy and stratigraphy of the Lunar South Pole-Aitken basin determined from Clementine UV/VIS and NIR data. Planetary and Space Science 68 (1),76e85.

23. Dhingra, D., (2008). Exploring links between crater floor mineralogy and layered lunar crust. Adv. Space Res. 42 (2), 275–280. doi:10.1016/j.asr.2007.10.024

24. V.sivakumar, R.Neelakanthan, M santosh (2016).Lunar surface minerology using hyperspectral data :Implication for primordial crust in the earth –moon system./Geoscience Frontiers 8(2017)457-465

25. Clark, R.N., Roush, T. L., (1984). Reflectance spectroscopy: quantitative analysis techniques for remote sensing applications. Journal of Geophysical Research: SolidEarth (1978e2012) 89 (B7), 6329e6340.

26. Clark, R.N., King, T.V.V., Gorelick, N.S., (1987). Automatic continuum analysis of reflectance spectra. In: Proceedings, Third AIS Workshop, 2e4 June, 1987, JPL Publication 87e30. Jet Propulsion Laboratory, Pasadena, California, pp. 138e142.

27. Cloutis, E.A., Sunshine, J.M., Morris, R.V., (2004). Spectral reflectance-compositionalproperties of spinels and chromites: implications for planetary remote sensing and geothermometry. Meteoritics and Planetary Science 39 (4), 545e566.

28. Pathak, S., Singh, R., Chauhan, M., Bhattacharya, S., Chauhan, P., (2015). Remote observation of lunar crater Hayn for mineralogical analysis using datasets from recent lunar missions. In: European Planetary Science Congress 2015, EPSC Abstracts 10. EPSC2015e559.

29. Pieters, C.M., Hanna, K.D., Cheek, L., Dhingra, D., Prissel, T., Jackson, C., Taylor, L.A., (2014). The distribution of Mg-spinel across the Moon and constraints on crustal origin. The second conference on the lunar highlands crust and new directions. American Mineralogist 99 (10), 1893e1910.

30. Isaacson, P.J., Pieters, C.M., Besse, S., Clark, R.N., Head, J.W., Klima, R.L., Mustard, J.F.,Petro, N.E., Staid, M.I., Sunshine, J.M., Taylor, L.A., Thaisen, K.G., Tompkins, S., (2011). Remote compositional analysis of lunar olivine-rich lithologies with Moon Mineralogy Mapper (M3) spectra. Journal of Geophysical Research: Planets (1991e2012) 116. E00G11.